Surface Science 678 (2018) 143–148

Contents lists available at ScienceDirect

Surface Science

journal homepage: www.elsevier.com/locate/susc

Amino acid nanopatterning on graphite

Eric Krebs, Linda Grabill, Andreas Riemann*

Department of Physics and Astronomy, Western Washington University, Bellingham, WA 98225, United States

ARTICLE INFO

Keywords:
Histidine
Tyrosine
Graphite
STM
Molecular mechanics
AMBER *ff03*

ABSTRACT

The present study provides an experimental and computational insight into amino acid adsorption on a graphite substrate. We investigated two aromatic amino acids, histidine and tyrosine, and their behavior on highly-ordered pyrolytic graphite (HOPG). The study was carried out under ambient conditions, in a 1-octanol solution and at room temperature. We found that both amino acids form well-ordered molecular films on graphite, as opposed to dimer rows found for another amino acid (methionine). Scanning Tunneling Microscopy reveals intermolecular spacings and angular orientations of the individual molecules in the well-ordered molecular layer. Both amino acids arrange themselves into a chevron pattern governed by inter-molecular attractive forces. The configuration consists of adjacent rows of parallel molecules, however, individual molecules in neighboring rows are angled with respect to each other. Additional computational chemistry methods using a Molecular Mechanics approach and the AMBER *ff03* force field are employed in support of the experimental findings. These calculations provide suggested molecular geometries and estimated adsorption energies and inter-molecular binding energies for molecules on a graphene sheet.

1. Introduction

A thorough understanding of the interactions between surfaces and adsorbates has the potential for manufacturing suitable functional structures at the nanometer scale to be used in molecular electronics, sensor technology, and medical applications [1,2]. In the last 30 years many approaches for this undertaking have been suggested and explored. With the development and/or improvement of various surface science techniques such as Scanning Tunneling Microscopy (STM), Atomic Force Microscopy (AFM), Spot Profile Analysis Low-Energy Electron Diffraction (SPA-LEED), X-Ray Photoelectron Spectroscopy (XPS) or Auger Electron Spectroscopy (AES) better experimental results have been obtained which then can be used to improve computational modeling of these data and therefore expand the overall understanding of the adsorbate-substrate interactions [3–8].

With advancements in experimental techniques, various kinds of adsorbates have been opened up for new investigations such as single atoms and molecules, alkali halides, pentacenes, biphenyls, porphyrins, ice molecules, amino acids, azobenzenes, and spiropyran-based molecular switches [9–23]. However, not only has it been possible to analyze the behavior of these adsorbates on substrates, but new artificially created structures could be constructed such as corrals or nanowires consisting of a few atoms/molecules up to micrometer length in size [24–28]. With that approach, macroscopic phenomena, such as Snell's law or standing waves patterns, could be verified as occurring on the surface of nanostructured materials as well [29–33].

Carbon-based substrates such as graphite, graphene and single-walled carbon nanotubes are an important class of template for the use in electronics and chemical sensors [34–36]. Adding biomolecules on the substrate allows for a modification of the substrate to obtain desirable properties. Here, amino acids play an important role to functionalize surfaces to be used for sensing applications and high adsorption capacity adsorbents [37–39].

Our study involved the adsorption of amino acids on a graphite substrate analyzed with STM under ambient conditions. The physical investigation was complimented with a Molecular Mechanics (MM) approach using a graphene sheet as a simplified template and to determine adsorption geometries and energies.

2. Method and model

In this study we used two amino acids (AA), namely histidine and tyrosine. Schematic models of these two AA can be seen in Fig. 1. The side chains of these AA are characterized by aromatic rings: Tyrosine has a benzene ring with an attached hydroxyl group, and histidine has an imidazole side chain containing two nitrogen atoms in the aromatic ring.

The experiments in this study were carried out with a home-built Scanning Tunneling Microscope using RHK electronics, and working under ambient conditions, at atmospheric pressure and room

* Corresponding author.
E-mail address: andreas.riemann@wwu.edu (A. Riemann).

https://doi.org/10.1016/j.susc.2018.04.013
Received 27 January 2018; Received in revised form 17 April 2018; Accepted 23 April 2018
Available online 05 May 2018

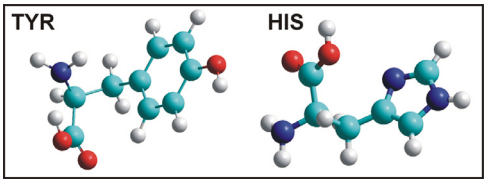

Fig. 1. Schematic model of the two amino acids, tyrosine (left) and histidine (right). (red - oxygen, black - nitrogen, turquoise - carbon, white - hydrogen). We will refer to the part of the amino acid with the carboxyl and amine groups as "head" and the side with the aromatic ring as the "tail", similar to our definition in a previous publication [40]. (For interpretation of the references to colour in this figure legend, the reader is referred to the web version of this article.)

temperature. A 0.25 mm PtIr wire was used as the scanning tip. The amino acid powders were mixed with 1-octanol solution at various mass concentrations between 0.005% and 0.24%. To ensure an even distribution of the amino acid in the liquid, the mixture was put in an ultrasonic bath for 5 to 10 min. A slab of highly ordered pyrolytic graphite (HOPG) with a 12 mm × 12 mm surface was prepared by acetone washing, baked in an open-air furnace for 5 min at 700 ° to remove any remaining residue, and finally cleaved to obtain a clean, well-established surface. 20 μL of the amino-acid/octanol solution was deposited onto the freshly cleaved graphite substrate immediately after cleaning. Amounts significantly larger than 20 μL of the solution led to situations where the surface structure could not be imaged due to multilayer configurations and interactions between tip and molecular film. The STM images were obtained with tunneling parameters of 1–3 nA and voltages of 0.2–0.5 V applied to the STM tip. The STM tip plunges through the covering, non-conducting octanol solution and images the adsorbed amino acid structures on the graphite substrate. STM images were processed using the software package WSXM [41]. Topographic images were edited by applying low-pass filters to remove noise from external vibrations. Distances in STM images were calibrated by using the HOPG substrate and its known surface geometry.

For the computational analysis, a combination of Density Functional Theory (DFT) and Molecular Mechanics was employed. Previous studies of molecule adsorption on carbon nanotubes have shown that this approach leads to successfully determining adsorption geometries and energies [42]. Molecules were geometry-optimized and frequency-checked at the B3LYP/ 6-31G++ level of theory using Gaussian 9.0 [43]. After determining that there were no imaginary frequencies (corresponding to physically improbable situations) atomic charges were generated at the same level of theory and basis set. In order to model the substrate, we choose graphene as a single layer instead of a multi-layer template which would be closer to our experimental situation. The model substrate is a 60 Å × 60 Å single layer slab with a mean bond length of 1.43 Å. Previous investigations have shown that the impact of the edge atoms on the adsorption geometry can be mitigated by a sufficiently large slab which necessitate the 60 Å × 60 Å dimensions. However, this creates another challenge as we are, due to computational limitations, currently not able to add additional layers to our substrate and have to restrict this study to a single graphene layer. Clearly, the electronic properties of HOPG and the chosen computational template of a graphene sheet differ due to missing bonds to underlying layers which influences the atomic charge distribution. From previous investigations of molecular adsorption on carbon surfaces, there are competing interests of lateral size (edge effects) and layer structure. Pykal et al. suggest that adsorption energies on a single layer graphene (as used in our approach) are around ~ 10% higher than those on few-layered graphene [44]. Keeping this in mind, we chose the single layer approach and treat our computational results as a good first estimate and as a proof of concept. The substrate charges were generated using the Mulliken atomic charge generation at the DFTBA level of theory, Gaussian 09's analytical approach to DFTB. The MM

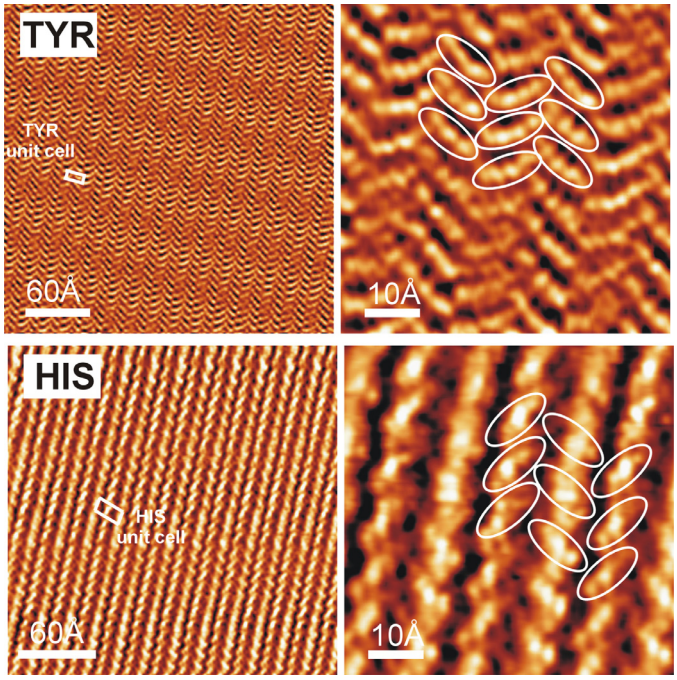

Fig. 2. Top: STM images of tyrosine film on graphite. Left: overview of molecular island (image size 300 Å × 300 Å). Right: Molecular configuration of individual molecules (image size: 60 Å × 60 Å). Tunneling parameters for both top view graphs: V = 370 mV, I = 1.01 nA. Bottom: STM images of histidine film on graphite. Left: overview of molecular island (image size 250 Å × 250 Å). Right: Molecular configuration (image size 60 Å × 60 Å). Tunneling parameters for bottom view graphs: V = 359 mV, I = 1.02 nA. Lateral calibration of the STM images was carried out using the clean HOPG substrate.

calculations were performed using the software package HyperChem 8.0.1 [45]. Carrying out the entire calculations using first principles methods proved to be not suitable for this system, since energy calculations of single points would take time in the order of minutes, and we carried out more than 5 million single point calculations with HyperChem. Previous studies on amino acids have shown that the force field AMBER *ff03* is a very suitable force field for graphite-amino acid calculations [42,46]. Using the optimized substrate and molecules we carried out calculations of adsorption energy, geometry, and total energy of the molecule-substrate system in order to find the energetically most favorable configurations. We compared the results with our experimental data and with other, higher-level calculations on similar systems.

3. Results and discussion

3.1. STM results

Independent of the concentration of the amino acid in the octanol solution, both, tyrosine and histidine, were observed to arrange into well-ordered molecular films on the graphite sample (see Fig. 2). Clearly visible for both molecules are chevron patterns consisting of molecular rows of parallel molecules with an inter-molecular spacing of about 10.0 ± 0.5 Å for histidine and 7.0 ± 0.5 Å for tyrosine. These distances were obtained by averaging the measured distances of inter-molecular spacings in various rows, and expressing the distance as $d_{average} \pm \sigma_{stdev}$. Each molecule is imaged as an oval shape with an overall length of about 13.0 ± 0.5 Å. The neighboring rows also consist of molecules in parallel orientation, however, the molecules are angled with respect to their adjacent row neighbors, creating the apparent chevron structure. The angle for tyrosine molecules is about

115 ± 10 °, for histidine 100 ± 10 °. The left view graphs show more clearly the repeating molecular structure with additional charge modulation in the molecules depicted as different contrast in the STM image. Since these images are recorded in constant current mode, the change in contrast caused by a vertical movement of the scanning tip can be interpreted as a proxy for a change in conductivity within the molecule. Overall, this well-ordered molecular film can be observed over wide areas of the graphite surface. The approach of depositing a droplet of AA/octanol solution onto the graphite crystal practically covers the whole sample. During STM imaging of clean and flat sample areas no clean graphite was found; so boundaries of the molecular film could not be identified. The structure is independent of the concentration, and in stark contrast to previously reported results for another amino acid, namely methionine, where, dependent on the concentration, molecular dimer rows with adjustable spacings could be observed [40]. The main reason for the adsorption behavior can be seen in the side chain of the different amino acid molecules: Whereas methionine has a side chain including sulfur, and a small dipole moment of 1.07 D (calculated using B3LYP/6-31G + +), the other two amino acids, tyrosine (2.79 D) and histidine (5.29 D), consist of an aromatic ring creating a larger dipole, as also confirmed by other studies [47,48]. The size of the dipole indicates the polar nature of the molecule which can have an influence on the inter-molecular forces and therefore on the inter-molecular orientations such as preferred “head-head”-interactions vs. “head-tail” interactions. Our previous experimental results using methionine, supported by molecular mechanics calculations, suggested a configuration where the amino acid heads (with methyl and amine groups) are attracted to each other, and the tails (side chain including sulfur) are repulsive, therefore creating dimer rows which are spaced further (repelled) when the amino acid concentrations are lower on the substrate [40,46]. In our present case, though, this repulsive behavior is not observed; we are postulating an overall attractive behavior between the heads and tails of the amino acids. Here, a change in concentration probably led to different molecular island sizes or different island densities. However, we were not able to determine the size of these islands since they appear larger than the maximum scanning range of our STM. Most likely the islands are limited in size by macroscopic features such as domain boundaries or area of cleanly cleaved graphite. Looking at the computational results will give us greater insight into the inter-molecular behavior.

3.2. Computational chemistry calculations

As described above, our calculations were carried out as a two-step process with the first step optimizing the substrate and molecules using higher level *ab initio* calculations and subsequently employing molecular mechanics calculations to determine adsorption geometries and energies. All calculations were carried out in vacuo. After optimizing the molecule using Gaussian 09, the tyrosine and histidine molecules, respectively, were positioned near the graphene substrate and the optimal, lowest energy configuration was calculated by letting the molecule interact with the substrate via the chosen force field. With this approach, we determined an adsorption energy of 0.87 eV (20 kcal/mol) for tyrosine and 0.79 eV (18 kcal/mol) for histidine, consistent with other studies of amino acids on carbon substrates [42,49,50]. In addition to the adsorption energies, we also investigated the geometry of the adsorption using Molecular Mechanics and the AMBER *ff03* force field (see Fig. 3). Looking at the tyrosine molecule, the aromatic, benzene ring is basically parallel to the substrate, most likely due to preferred parallel stacking of benzene rings of the substrate and molecule, in this case very close to an AB stacking geometry. On the other hand, as evident for histidine the aromatic, imidazole ring is basically perpendicular to the graphene sheet. Previous first principles calculations, such as Density Functional Theory with Local Density Approximation (DFT-LDA) and DFT-Generalized Gradients Approximation by Perdew, Burke and Ernzerhof (GGA-PBE) found identical geometries [49].

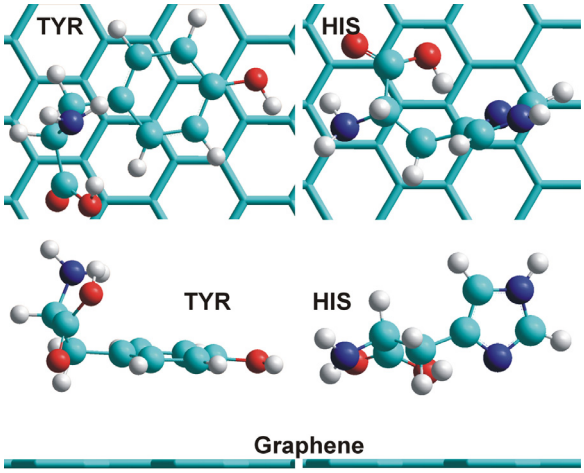

Fig. 3. Adsorption geometry for tyrosine (left) and histidine (right) in top view (top) and side view (bottom).

The experimental data clearly show that both amino acids are arranged on the surface in a film structure and not as dimer rows, which was observed for another amino acid (methionine) [40]. Therefore, the first investigation was about the behavior of molecules in parallel and in anti-parallel orientation (see Fig. 4). In order to investigate the interactions of two amino acid molecules on the substrate, we fixed one adsorbed molecule on the substrate (at the origin of our coordinate system, see central molecule in all graphs of Fig. 4) and added a second molecule which we moved around the substrate in a predetermined way as follows: The lateral step size was 0.1 Å in both horizontal dimensions (parallel to the graphene sheet) on a 30 Å × 30 Å grid, and the angular rotation step size was 15° with respect to a rotation axis perpendicular to the substrate. These calculations lead to about 2 million energy values for the adsorption of a second molecule. Fig. 4 shows the energy maps due to lateral motion of the secondary molecule when positioned at angles of 0° (parallel) and 180° (anti-parallel), respectively, with respect to the stationary central molecule. When both molecules are parallel to each other, the energy maps show that areas of lowest energy (indicated red in Fig. 4) are located where these molecules are oriented in a head-to-tail fashion with the head where the carboxyl and amine groups are and the tail where the aromatic ring is. This result is noticeably different than previous studies with the amino acid methionine [40]. There the repulsion of the head and tail of the amino acid leads to the formation of molecular wires compromised of dimers in head-to-head configuration. The left two graphs of Fig. 4 show the molecules in parallel orientation and the two graphs on the right in anti-parallel orientation. Both graphs relay the same information: opposite ends of the amino acids are attractive (have a lower energy as seen in the left graphs) and same ends are repulsive (low energy can be found when molecules are positioned next to each other instead of facing each other, as seen in the right graphs). Therefore, this attractive interaction between head and tail ultimately leads to the observed film growth of the molecular adsorbates. Looking at the configuration within the rows where the AA molecules are parallel, the geometry is driven by a combination of intermolecular attraction and the periodicity of the underlying substrate with both effects contributing to the total binding energies. Regarding spacing of molecules, the energy map for two tyrosine molecules parallel to each other reveals a minimum spacing of about 7.0 ± 0.5 Å (indicated by the borders of the deep purple region in Fig. 4) consistent with our experimental findings. For histidine, the energy map for the parallel configuration leads to a spacing of about 7.5 ± 0.5 Å, about 20% less than the experimental findings. In general, our calculations match the adsorption geometries of parallel molecules deduced from the STM images (see left viewgraphs in Fig. 2), though, fairly well.

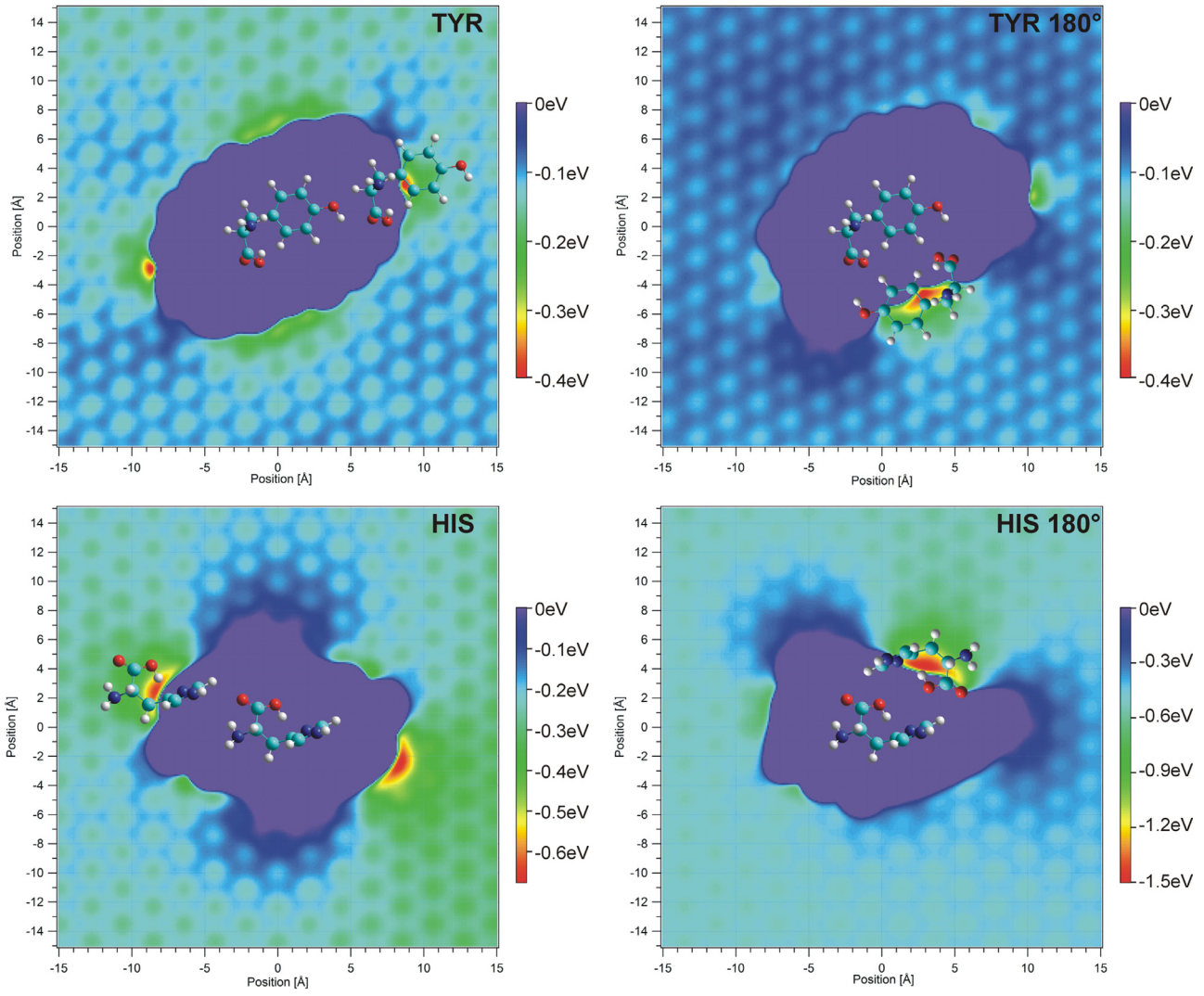

Fig. 4. Energy map of tyrosine (top) and histidine (bottom) in parallel (left) and anti-parallel (right) configuration. Deep purple areas around the origin are energetically very unfavorable, molecules basically overlap in this area. Red areas, though, indicate lowest energy configurations. Top left: Tyrosine molecules in parallel orientation with lowest energy due to attraction between head and tail of AA. Binding energy of 0.24 eV (5.6 kcal/mol). Top right: Tyrosine molecules in anti-parallel orientation not showing attraction between same-side ends of molecule, therefore molecules in anti-parallel configuration are positioned next to each other with 0.39 eV (9.0 kcal/mol) energy. Bottom left: Histidine molecules in parallel orientation with lowest energy due to attraction between head and tail of AA. Binding energy of 0.38 eV (8.7 kcal/mol). Bottom right: Histidine molecules in anti-parallel orientation not showing attraction between same-side ends of molecule, molecules in anti-parallel configuration located next to each other with 0.85 eV (19.5 kcal/mol) energy. (For interpretation of the references to colour in this figure legend, the reader is referred to the web version of this article.)

In order to evaluate the geometry of the chevron structure of the molecular film observed in the STM images, we used the approach of allowing the secondary molecule to rotate in pre-determined steps around an axis perpendicular to the substrate and move laterally on the same 30 Å × 30 Å grid as before. These calculations resulted in intermolecular binding energies of up to 0.5 eV for tyrosine and up to 0.9 eV for histidine. For tyrosine molecules using the angle of 115 ± 10° resulted in a binding energy of about 0.4 ± 0.1 eV. Using histidine with the experimentally determined angle between molecules in adjacent rows of 100 ± 10° yielded a binding energy of 0.4 ± 0.1 eV for these neighboring molecules. Our calculations show that it is energetically favorable for molecules in adjacent rows to be angled in such a way that the "tail" (the side chain with the aromatic ring) is close to the "head" (the amine and carboxyl groups) of the AA molecule (see Fig. 5). Our results for energy are consistent with previous other studies of amino acid interactions [51,52]. As mentioned before, the adsorption geometries and energies are driven by a combination of inter-molecular forces and molecule-substrate interactions. Our model of a single sheet graphene substrate could under- or overestimate the molecule/substrate interactions as compared to the experimentally used graphite surface. However, qualitative and quantitative results related to adsorption geometry and energy can be deduced from the calculations.

Rahsepar et al. describe in their work the nature of the interactions of amino acids when adsorbed on a substrate [53]. The suggestion of substrate-mediated hydrogen bonds resulting in a bond length of about 1.7 Å and an energy of 7.2 kcal/mol (0.31 eV) for methionine and O-H···O bonds, are comparable to our results and indicate similar intermolecular interactions for amino acids used in the present study.

4. Conclusion

Using the amino acids histidine and tyrosine consisting of aromatic rings in their side chain, we found that these molecules form a well-ordered film when adsorbed on graphite. A regular chevron-shaped structure can be observed with rows of parallel molecules where molecules in adjacent rows are angled. The individual molecules in these

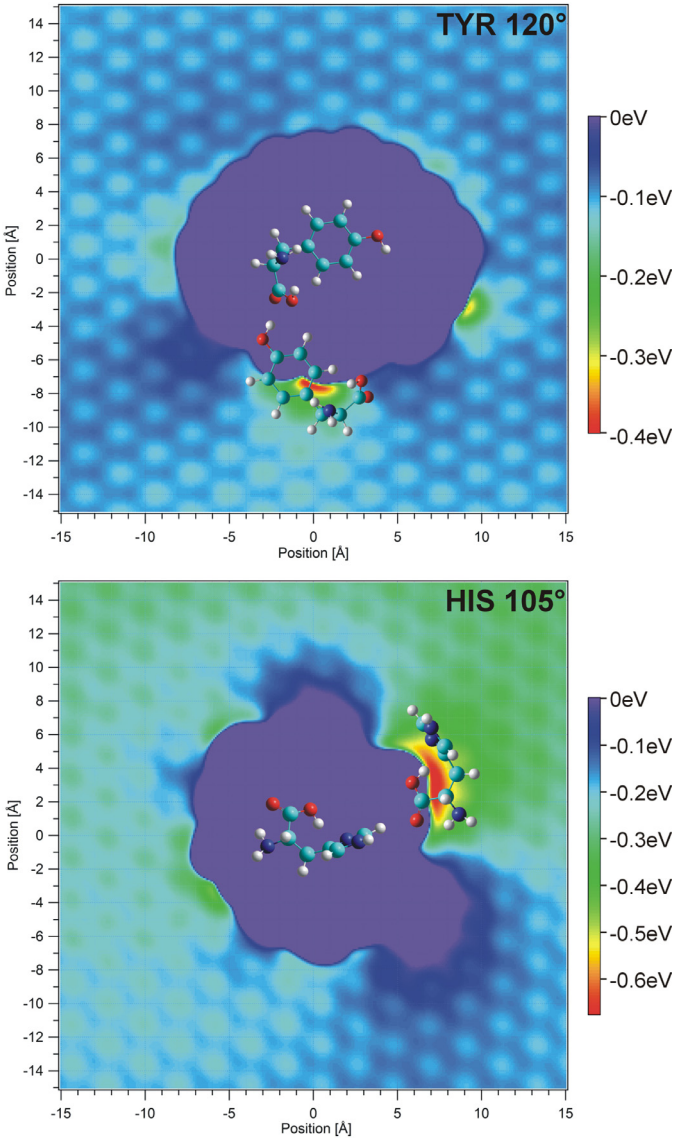

Fig. 5. Orientation of angled molecules. Top: Two tyrosine molecules at an angle of 120° with a binding energy of 0.40 eV (9.1 kcal/mol). Bottom: Two histidine molecules at an angle of 105°. The binding energy in this case is 0.42 eV (9.6 kcal/mol).

rows are separated by 7.0 ± 0.5 Å, and next-row neighboring molecules are angled at about 115 ± 10° for tyrosine, whereas the values for histidine are: 10.0 ± 0.5 Å and 100 ± 10°. Computational Chemistry calculations using a graphene sheet as substrate and the two AA molecules as adsorbate yield adsorption energies of 0.87 eV and 0.79 eV for tyrosine and histidine, respectively. These qualitative results are comparable to other higher level studies on amino acids [52]. Furthermore, we could identify the underlying self-assembly principle with these computational molecular mechanics calculations: An attractive interaction between the two ends of the amino acid was found which leads to the observed film growth. These findings are different than the dimer growth found previously for a different amino acid, namely methionine [40]. The MM calculations found inter-molecular binding energies of about 0.4 ± 0.1 eV for tyrosine and for histidine. Comparing the present study and the results here-in using aromatic amino acids with a previous study of the amino acid methionine (MET) with sulfur in its side chain, we conclude that the side chain is responsible for the growth mechanism on the substrate, be it film growth (HIS & TYR) or row structures (MET).

For follow-up investigations of the amino acid/carbon substrate study and in order to enhance the quantitative approach using computational chemistry methods, a substrate with multiple layers of interacting graphene sheets could be used as template. However, this approach would lead to a large increase in computational resources currently not feasible by the authors.

Supplementary material

Supplementary material associated with this article can be found, in the online version, at doi:10.1016/j.susc.2018.04.013.

References

[1] J.M. MacLeod, F. Rosei, Molecular self-assembly on graphene, Small 10 (2014) 1038.
[2] R. Gatti, J.M. MacLeod, J.A. Lipton-Duffin, A.G. Moiseev, D.F. Perepichka, F. Rosei, Substrate, molecular structure, and solvent effects in 2D self-assembly via hydrogen and holgen bonding, J. Phys. Chem. C 118 (2014) 25505.
[3] G. Binnig, H. Rohrer, C. Gerber, E. Weibel, Surface studies by scanning tunneling microscopy, Phys. Rev. Lett. 49 (1982) 57.
[4] G. Binnig, H. Rohrer, C. Gerber, E. Weibel, Tunneling through a controllable vacuum gap, Appl. Phys. Lett. 40 (1982) 47.
[5] G. Binnig, C.F. Quate, C. Gerber, Atomic force microscope, Phys. Rev. Lett. 56 (1986) 930.
[6] U. Scheithauer, G. Meyer, M. Henzler, A new LEED instrument for quantitative spot profile analysis, Surf. Sci. 178 (1986) 441.
[7] K. Bierbaum, M. Kinzler, C. Wöll, M. Grunze, G. Hähner, S. Heid, F. Effenberger, A near edge x-ray absorption fine structure spectroscopy and x-ray photoelectron spectroscopy study of the film properties of self-assembled monolayers of organosilanes on oxidized si(100), Langmuir 11 (1995) 512.
[8] P. Weightman, X-Ray-excited auger and photoelectron spectroscopy, Rep. Progr. Phys. 45 (1982) 753.
[9] L. Bartels, G. Meyer, K.-H. Rieder, D. Velic, E. Knoesel, A. Hotzel, M. Wolf, G. Ertl, Dynamics of electron-induced manipulation of individual CO molecules on cu(111), Phys. Rev. Lett. 80 (1998) 2004.
[10] S.-W. Hla, L. Bartels, G. Meyer, K.-H. Rieder, Inducing all steps of a chemical reaction with the scanning tunneling mircoscope tip: towards single molecule engineering, Phys. Rev. Lett. 85 (2000) 2777.
[11] F. Moresco, G. Meyer, K.-H. Rieder, H. Tang, A. Gourdon, C. Joachim, Conformational changes of single molecules induced by scanning tunneling microscopy manipulation: a route to molecular switching, Phys. Rev. Lett. 86 (2001) 672.
[12] F. Moresco, G. Meyer, K.-H. Rieder, J. Ping, H. Tang, C. Joachim, Tbpp molecules on copper surfaces: a low temperature scanning tunneling microscope investigation, Surf. Sci. 499 (2002) 94.
[13] K. Morgenstern, K.-H. Rieder, Formation of the cyclic ice haxamer via excitation of vibrational molecular modes by the scanning tunneling microscope, J. Chem. Phys. 116 (2002) 5746.
[14] A. Riemann, S. Fölsch, K.H. Rieder, Epitaxial growth of alkali halides on stepped metal surfaces, Phys. Rev. B 72 (2005) 125423.
[15] J. Repp, S. Fölsch, G. Meyer, K.-H. Rieder, Ionic films on vicinal metal surfaces: enhanced binding due to charge modulation, Phys. Rev. Lett. 86 (2001) 252.
[16] J. Lagoute, K. Kanisawa, S. Fölsch, Manipulation and adsorption-site mapping of single pentacene molecules on Cu(111), Phys. Rev. B 70 (2004) 245415.
[17] J. Repp, G. Meyer, S. Paavilainen, F.E. Olsson, M. Persson, Imaging bond formation between a gold atom and pentacene on an insulating surface, Science 312 (2006) 1196.
[18] L. Grill, K.-H. Rieder, F. Moresco, G. Rapenne, S. Stojkovic, X. Bouju, C. Joachim, Rolling a single molecular wheel at the atomic scale, Nat. Nanotechn. 2 (2007) 95.
[19] M. Alemani, M.V. Peters, S. Hecht, K.-H. Rieder, F. Moresco, L. Grill, Electric field-induced isomerization of azobenzene by STM, J. Am. Chem. Soc. 128 (2006) 14446.
[20] F. Chiaravalloti, L. Gross, K.-H. Rieder, S.M. Stojkovic, A. Gourdon, C. Joachim, F. Moresco, A rack-and-pinion device at the molecular scale, Nat. Mat. 6 (2007) 30.
[21] M. Alemani, S. Selvanathan, F. Ample, M.V. Peters, K.-H. Rieder, F. Moresco, C. Joachim, S. Hecht, L. Grill, Adsorption and switching properties of azobenzene derivatives on different noble metal surfaces: Au(111), Cu(111), and Au(100), J. Phys. Chem. C 112 (2008) 10509.
[22] M. Piantek, G. Schulze, M. Koch, K.J. Franke, F. Leyssner, A. Krüger, C. Navío, J. Miguel, M. Bernien, M. Wolf, W. Kuch, P. Tegeder, J.I. Pascual, Reversing the thermal stability of a molecular switch on a gold surface: ring-opening reaction of nitrospiropyran, J. Am. Chem. Soc. 131 (2009) 12729.
[23] A. Schiffrin, A. Riemann, W. Auwärter, Y. Pennec, A. Weber-Bargioni, D. Cvetko, A. Cossaro, A. Morgante, J.V. Barth, Zwitterionic self-assembly of L-methionine nanogratings on the Ag(111) surface, Proc. Nat. Acad. Sci. 104 (2007) 5279.
[24] M.F. Crommie, C.P. Lutz, D.M. Eigler, Confinement of electrons to quantum corrals on a metal surface, Science 262 (1993) 218.
[25] A.T. Ngo, E.H. Kim, S.E. Ulloa, Single-atom gating and magnetic interactions in quantum corrals, Phys. Rev. B 95 (2017) 161407(R).
[26] Y. Yu, J. Sun, P. Yang, Atomic structure of ultrathin gold nanowires, Nano Lett. 16 (2016) 3078.

[27] M.E.T. Molares, V. Buschmann, D. Dobrev, R. Neumann, R. Scholz, I.U. Schuchert, J. Vetter, Single-crystalline copper nanowires produced by electrochemical deposition in polymeric ion track membranes, Adv. Mater. 13 (2001) 62.
[28] T. Kang, I. Yoon, J. Kim, H. Ihee, B. Kim, Au nanowireau nanoparticles conjugated system which provides micrometer size molecular sensors, Chem. Eur. J. 16 (2010) 1351.
[29] S.-W. Hla, K.-F. Braun, K.-H. Rieder, Single-atom manipulation mechanisms during a quantum corral construction, Phys. Rev. B 67 (2003) 201402.
[30] J. Repp, G. Meyer, K.-H. Rieder, Snell's law for surface electrons: refraction of an electron gas imaged in real space, Phys. Rev. Lett. 92 (2004) 036803.
[31] K.-H. Rieder, G. Meyer, S.-W. Hla, F. Moresco, K.F. Braun, K. Morgenstern, J. Repp, S. Fölsch, L. Bartels, The scanning tunnelling microscope as an operative tool: doing physics and chemistry with single atoms and molecules, Philos. Trans. R. Soc. 362 (2004) 1207.
[32] K.-F. Braun, K.-H. Rieder, Engineering electronic lifetimes in artificial atomic structures, Phys. Rev. Lett. 88 (2002) 096801.
[33] J. Lagoute, S. Fölsch, Interaction of single pentacene molecules with monatomic Cu/ Cu(111) quantum wires, J. Vac. Sci. Technol. B 23 (2005) 1726.
[34] C. Cheng, S. Li, A. Thomas, N.A. Kotov, R. Haag, Functional graphene nanomaterials based architectures: biointeractions, fabrications, and emerging biological applications, Chem. Rev. 117 (2017) 1826.
[35] G. Reina, J. González-Domínguez, A. Criado, E. Vásquez, A. Bianco, M. Prato, Promises, facts and challenges for graphene in biomedical applications, Chem. Soc. Rev. 468 (2017) 4400.
[36] Q. Quan, X. Lina, N. Zhang, Y.-J. Xu, Graphene and its derivatives as versatile templates for materials synthesis and functional applications, Nanoscale 9 (2017) 2398.
[37] S.J. Rodríguez, L. Makinistian, E. Albanesi, Graphene for amino acid biosensing: theoretical study of the electronic transport, Appl. Surf. Sci. 419 (2017) 540.
[38] D. Shu, F. Feng, H. Han, Z. Ma, Prominent adsorption performance of amino-functionalized ultralight graphene aerogel for methyl orange and amaranth, Chem. Eng. J. 324 (2017) 1.
[39] A. Maleki, U. Hamesadeghi, H. Daraei, B. Hayati, F. Najafi, G. McKay, R. Rezaee, Amine functionalized multi-walled carbon nanotubes: single and binary systems for high capacity dye removal, Chem. Eng. J. 313 (2017) 826.
[40] A. Riemann, B. Nelson, Molecular wires self-assembled on a graphite surface, Langmuir 25 (2009) 4522.
[41] I. Horcas, R. Fernández, J.M. Gómez-Rodríguez, J. Colchero, J. Gómez-Herrero, A.M. Baro, Wsxm: a software for scanning probe microscopy and a tool for nanotechnology, Rev. Sci. Instr. 78 (2007) 013705.
[42] L. Grabill, A. Riemann, Conformational impact on amino acid-surface $\pi - \pi$ interactions on a (7,7) single walled carbon nanotube: a molecular mechanics approach, J. Phys. Chem. A 122 (2018) 1713.
[43] M.J. Frisch, G.W. Trucks, H.B. Schlegel, G.E. Scuseria, M.A. Robb, J.R. Cheeseman, G. Scalmani, V. Barone, B. Mennucci, G.A. Petersson, H. Nakatsuji, M. Caricato, X. Li, H.P. Hratchian, A.F. Izmaylov, J. Bloino, G. Zheng, J.L. Sonnenberg, M. Hada, M. Ehara, K. Toyota, R. Fukuda, J. Hasegawa, M. Ishida, T. Nakajima, Y. Honda, O. Kitao, H. Nakai, T. Vreven, J.A. Montgomery, Jr., J.E. Peralta, F. Ogliaro, M. Bearpark, J.J. Heyd, E. Brothers, K.N. Kudin, V.N. Staroverov, T. Keith, R. Kobayashi, J. Normand, K. Raghavachari, A. Rendell, J.C. Burant, S.S. Iyengar, J. Tomasi, M. Cossi, N. Rega, J.M. Millam, M. Klene, J.E. Knox, J.B. Cross, V. Bakken, C. Adamo, J. Jaramillo, R. Gomperts, R.E. Stratmann, O. Yazyev, A.J. Austin, R. Cammi, C. Pomelli, J.W. Ochterski, R.L. Martin, K. Morokuma, V.G. Zakrzewski, G. A. Voth, P. Salvador, J.J. Dannenberg, S. Dapprich, A.D. Daniels, O. Farkas, J.B. Foresman, J.V. Ortiz, J. Cioslowski, D.J. Fox, *Gaussian 09*, Revision D.01, 2009. Gaussian, Inc.: Wallingford, CT, 2009.
[44] M. Pykal, P. Jurečka, F. Karlický, M. Otyepka, Modelling of graphene functionalization, Phys. Chem. Chem. Phys. 18 (2016) 6351.
[45] Hypercube, Inc., *HyperChem(TM) Professional 8.0.10*, 2007, (Hypercube, Inc.: Gainesville, Florida, 2007).
[46] B. Owens, A. Riemann, A computational analysis for amino acid adsorption, Surf. Sci. 624 (2014) 118.
[47] B. Dittrich, D. Jayatilaka, Reliable measurements of dipole moments from single-crystal diffraction data and assessment of an in-crystl enhancement, Struct. Bond. 147 (2012) 27.
[48] J. Setiadi, S. Kuyucak, Elucidation of the role of a conserved methionine in glutamate transporters and its implication for force fields, J. Phys. Chem. B 121 (2017) 9526.
[49] S.J. Rodríguez, L. Makinistian, E. Albanesi, Theoretical study of the adsorption of histidine amino acid on graphene, J. Phys. Conf. Ser. 705 (2016) 012012.
[50] T. Roman, W.A. Dino, H. Nakanishi, H. Kasai, Amino acid adsorption on single-walled carbon nanotubes, Eur. Phys. J. D 38 (1) (2006) 117.
[51] O. Markovitch, N. Agmon, Structure and energetics of the hydronium hydration shells, J. Phys. Chem. A 111 (2007) 2253.
[52] B. Dalhus, C.H. Görbitz, Crystal structures of hydrophobic amino acids: interaction energies of hydrogen-bonded layers revealed by ab initio calculations, J. Mol. Struct. (THEOCHEM) 675 (2004) 47.
[53] F.R. Rahsepar, N. Moghimi, K.T. Leung, Surface-mediated hydrogen bonding of proteinogenic α-amino acids on silicon, Acc. Chem. Res. 49 (2016) 942.